Final Report for 2014 USGS NEHRP Award G14AP00058
Correlation of Injection Induced Earthquake Swarms with Temporal Changes in Shear Velocity in the Salton Sea Geothermal Field?

Jeff McGuire
Dept. of Geology and Geophysics,
MS 24, Woods Hole Oceanographic Institution
Woods Hole MA 02543

Award Dates: 06/01/2014 – 12/31/2015

Abstract

Earthquake swarms provide a clear indication that there are distinct, relatively short time periods (days) when the physical criteria for fault failure are more easily met. However, we have very limited ability to measure the relevant physical properties of the fault-zone and the stress levels within it during these swarms. The high level of seismicity in the Salton Sea Geothermal Field (SSGF) and the dense borehole seismic network have allowed the P to identify the effects of fluid injection on both earthquake migration and source properties like stress-drop. Additionally, we have preliminary results that indicate changes in fault-zone material properties during injection-induced swarms. We analyze the temporal variability in the S-wave coda from earthquake multiplets. For the seismometer located within the damage zone of the main central fault, there is clear time dependence to the S-wave coda that indicates a drop in average S-velocity within the fault zone around late 2009. This drop in S-wave velocity was coincident with a drop in the average injection pressure at a cluster of nearby injection wells. Attempts to measure similar velocity changes at other stations within the field did not show any significant time dependence. Thus, the signal corresponding to the pressure drop appears to be localized within the fault-zone. The velocity drop is imagined during an earthquake swarm in January 2010 shortly after the drop in injection pressure. This is the clearest time-dependent signal in the ~6 year period for which the borehole seismic data is publically available. It suggests that such data, if it were routinely available, would help clarify the causative relationships between fluid injection patterns and the mechanics of earthquake nucleation.

Geological Setting. The Salton Sea Geothermal field (SSGF) is part of the Brawley Seismic zone. This region accommodates the transfer of the majority of PA-NA plate motion from the San Andreas Fault to the Imperial Fault. While the seismicity typically occurs within the sedimentary layers that fill the Salton Trough, the region of the geothermal field is likely underlain by a significant igneous intrusive body as evidenced by the bulls-eye gravity and magnetic anomalies high seismic velocities and a fairly localized temperature anomaly (>300 C at 900m) all coincident with the volcanic centers (Obsidian Butte, Rock Hill, and Red Island) located along the southern coast of the Salton Sea (Elders and Sass [1988] and references therein) (Figure 1). Numerous shallow geothermal exploration wells and one deep Continental Drilling project well (~3 km) have provided extensive information about the stratigraphy around the geothermal field. In general, the field is overlain by ~500m of impermeable cap rock comprised of unconsolidated clay, silt and gravel within which heat flow is high and primarily conductive [*Younker et al.*, 1982]. Between the cap rock and the base of the geothermal wells (typically 1000-2000m) are an "upper reservoir layer" of relatively unaltered sandstone with higher porosity and significant fracturing, and a "lower reservoir layer" of reduced porosity, hydrothermally altered sediments that have been metamorphosed into dense, highly-fractured albite-epidote hornfels [*Clayton et al.*, 1968] (Figure 2). The boundary between the cap rock and the reservoir is a strong boundary in seismic velocity and geothermal gradient [*Younker et al.*, 1982]. A smaller component of diabase sills and rhyollitic layers are also observed in some of the deeper portions of the reservoir rock [*Herzign et al.*, 1988; *Schmitt and Hulen*, 2008]. The reservoir is generally defined as the region where the shallow thermal gradient in the 30-80m depth range exceeds 200 °C/km [*J Hulen and Pulka*, 2001; *J B Hulen et al.*, 2002; *Newmark et al.*, 1988]. Some wells reach temperatures as high as 389 °C at 2km depth.

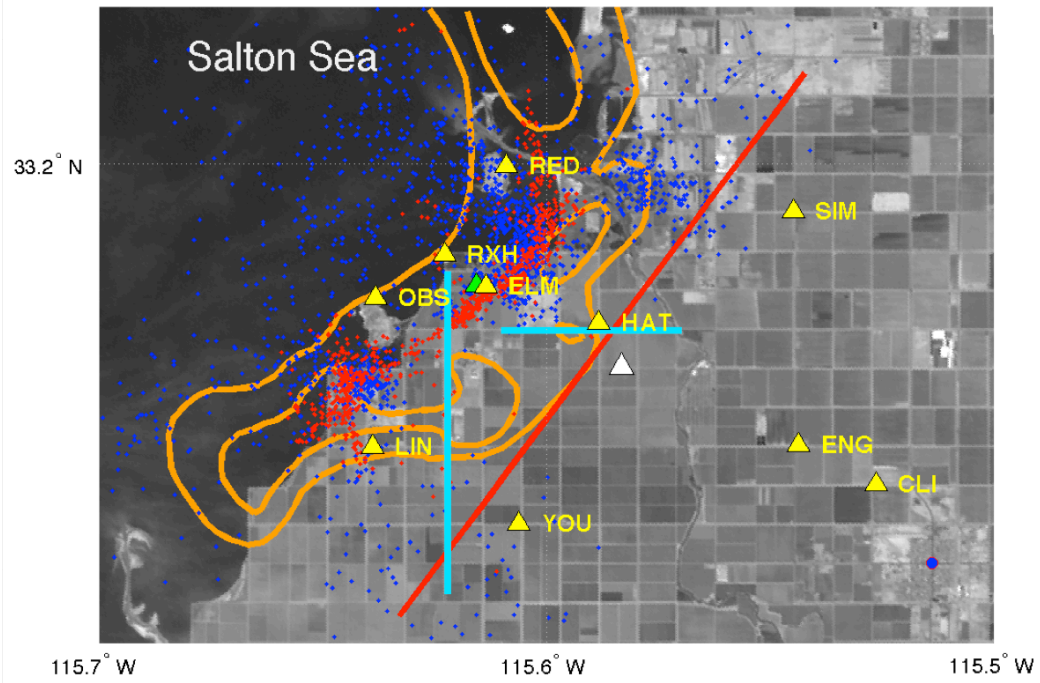

Figure 1. Map of the SSGF. Blue and red circles denote background seismicity and the 2005 swarm respectively. Light-blue lines denote active source seismic lines. Orange contours

denote the regions of high shallow thermal gradient [*J Hulen and Pulka*, 2001]. The outer contour corresponds to the 300 °C/km and denotes the limit of the reservoir, while the inner contours denote the 700 °C/km gradient and roughly denote the regions where extraction is significant. The yellow triangles denote the locations of the borehole seismic network. The red-line denotes the surface trace of the best-fit fault from inverting the InSAR data covering the 2005 swarm.

The SSGF is an immense operation in terms of fluid flow and unique for occurring at such a scale directly within a seismically active plate boundary zone. Fluid circulation within the reservoir is thought to be dominantly vertical rising of hot fluid, ~400 °C, along highly permeable fractures and faults. The geothermal wells typically tap into this fluid at depths of 1-2 km. The largest structural feature in the field is termed 'the main central fault' and is thought to be a ~10 km long left-lateral strike-slip fault and is a major zone of high permeability and upflow from the deeper resevoir [*J Hulen and Pulka*, 2001]. There are dozens of production wells, which generally exceed 1,000,000 lbs of brine/hour without any pumping. Some of the largest produce 45 MW of generation and have been flowing for 30 years at 3,000,000 lbs/hour with no significant drop in pressure. Injection wells can take up to 3 million pounds of fluid per hour without the need for any fracking. Essentially the well-head pressure of ~100 psi is enough to drive fluid into the highly permeable fractures at depth.

There is nearly constant seismic activity within the field (many earthquakes per day located by the SCSN) and it is loosely characterized as three types. There is diffuse background seismicity as well as are three dominant clusters of continuous background seismicity that are associated with major production and injection areas. This concentrated seismicity located between 1 and 2.5 km depth (blue circles in Figure 1). Additionally, in 2005 there was a large swarm of left-lateral strike slip events that initiated near station ELM and propagated bilaterally over ~10 km over the course of a day [*Lohman and McGuire*, 2007]. This earthquake swarm was associated with a large (~15 cm) surface scarp (white triangle in figure 1) and surface deformation signal detected by InSAR that corresponded to a Mw 5.7 creep event [*Lohman and McGuire*, 2007]. Over the last few years we have worked to investigate the complex network of faults in the SSGF and understand which structures were responsible for both the seismic swarm and the aseismic slip detected by InSAR. With new relocations of the 2005 seismicity using a 3D velocity model, it is clear that they occurred primarily within the highest temperature regions and essentially connect two of the major injection related clusters (Figure 1). They locate coincidentally with a large left-lateral strike-slip fault that has been imaged in geologic cross sections using well log data.

In 2010 USGS, WHOI, and Cornell conducted an active source seismic survey of two perpendicular lines within the SSGF to identify the fault structures associated with the 2005 swarm. There is a major multistranded fault system intersecting the N-S seismic line shown in Figure 1 in the northern half of the line. This fault system is spatial coincident with the left-lateral earthquake swarm in 2005 (see Figure 1). It is approximately 1 km wide. Unlike many fault-zones, this 'main central fault' actually occurs within the highest velocity material. The active source imaging found that shallow (0-2km) P-wave velocities were 30% higher in the northern half of the line than the southern half. We have combined the active source shots with differential arrival times from earthquake recordings on the CalEnergy borehole seismic network (Figure 1) to construct a 3D velocity model for the field. It demonstrates the very large (>30%) P-

wave anomalies are coincident with the regions of the highest temperatures. This ~1km wide fault-zone is best delineated by the 2005 swarm and trends NE-SW passing nearly through the borehole seismic station ELM (Figure 1). See [*Jeffrey J. McGuire et al.*, 2015] for detailed images of the fault-zone and its relationship to earthquake locations.

Fluid Injection Effects on Seismicity

Xiaowei Chen and Peter Shearer have documented several aspects of seismicity within the SSGF that indicate the influence of fluid injection on earthquake occurrence and source properties within the field [*Chen and Shearer*, 2011] and elsewhere [*Chen et al.*, 2012]. First, by computing earthquake source spectra and stress drop estimates for moderate M2+ earthquakes within the field since its inception in ~1981, they have documented a clear increase in stress drop with distance from active injection wells. This factor of two increase in stress drop likely indicates that the fluid injection is decreasing the overall effective stress by increasing the pore pressure in a ~2km radius around the injection wells. The magnitude of this change, ~0.4 MPa= 58 Psi is almost identical to a typical wellhead pressure in the SSGF (<= 100 Psi; A Schreiner, pers. comm.). This trend was even observed within the ~3 day long 2005 swarm with median stress drops increasing by about a factor of two between the beginning of the swarm and its end. This is particularly interesting, because while the 2005 swarm occurred primarily along a major tectonic fault, it initiated very close to (but ~1-2 km deeper) than the most active cloud of induced microseismicity (Figure 1).

Many of the injection wells are clustered very close to the main central fault as delineated by the 2005 swarm (Figure 2). The swarm occurred at ~2-5km depth and the wells, many of which are not vertical, likely intersect the fault-zone in the 1-2 km depth range. In particular, there is a clear build up in well pressure during 2009 that drops rapidly around January 2010. Unfortunately only monthly pressure data is available.

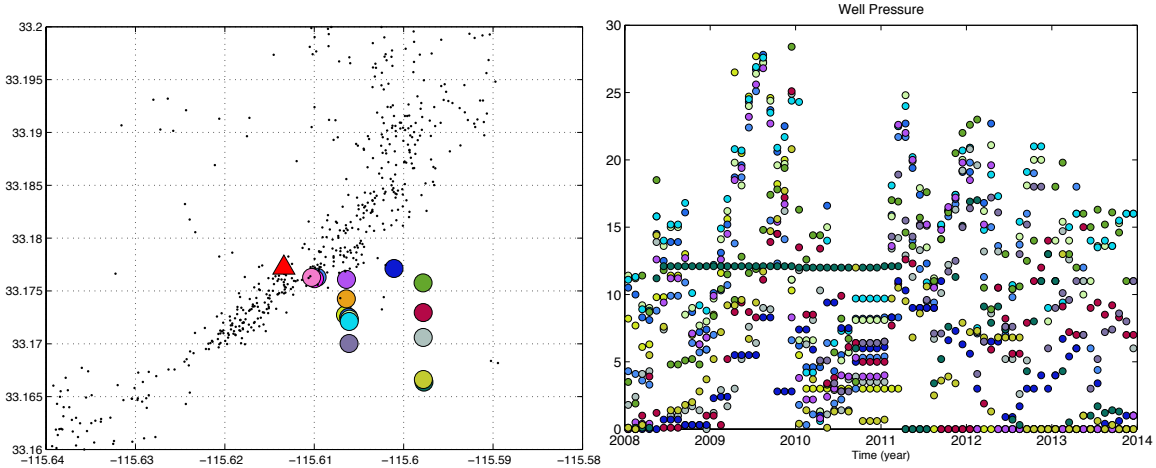

Figure 2. Left) Locations of a cluster of injection wells (colored circles) near the main central fault and station ELM (red triangle). The black dots denote the locaitons of the 2005 earthquake swarm from McGuire et al., 2015 which denotes the main strike-slip fault within the geothermal field. Right) Monthly time history of well pressure in each well as reported to DOGGR. The symbol colors correspond to the map on the right. There was a distinct drop in pumping in early 2010 at the time of a large earthquake swarm.

Velocity Change Measurements

We infer temporal changes in the fault zone material properties represented as relative changes (dv/v) in S-wave speed, from the time-dependent stretching of the S-wave coda (Figure 3) measured with a doublet method [*J. J. McGuire et al.*, 2012]. For each selected earthquake we determined a stretching coefficient by comparison against a reference signal, which was obtained by stacking waveforms from selected small earthquakes in a particular cluster (Figure 3). For details see McGuire et al. 2012.

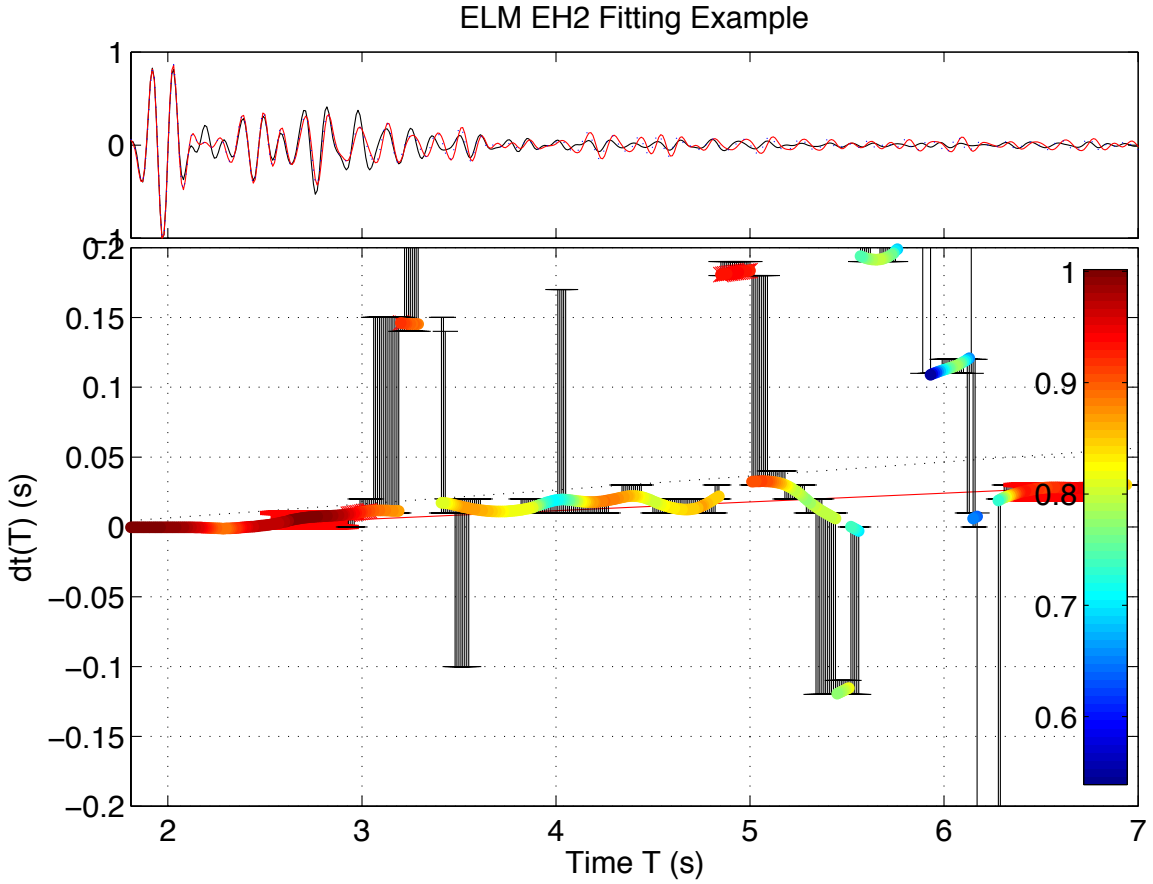

Figure 3. Example of a measurement of a velocity change at station ELM. The top panel shows the stack of all S-wave coda seismograms in the multiplet along with the seismogram for one particular earthquake in the January 2010 swarm. The bottom panel shows measurements of the relative time shift in short windows as a function of delay time T within the coda. Colors denote the correlation coefficient at each measurement.

We applied the same approach as in McGuire et al. 2012, but with many parameters adjusted to the length, frequency content, and other features of the S-wave coda at station ELM which is located extremely close to the main central fault (Figure 1). We evaluated one cluster of ~500 earthquakes located in the induced seismicity area just NE of station ELM. The drops in velocity happen extremely quickly (hours) during earthquake swarms in particular in January 2010 (corresponding to the discontinuities at

earthquake ~180). The recoveries back to the higher average velocity values have time scales of months during 2010 (figure 4). These changes are large enough to be easily visualized in a record section of the S-wave coda (Figure 5). Moreover, the velocity drop effected a significant volume of the fault-zone. It can be seen in coda arrivals as early as ~2.5 seconds on the x-axis in Figure 5 and as late as 4.5 seconds. Due to the source station geometry, all of this scattered energy likely spent the majority of its path in the fault-zone, albeit with different sensitivities as one looks later in the coda arrival. The observation that one dv/V value can predict the shifts in coda arrivals all the way out to 4.5 seconds (white lines in figure 5) indicates that the velocity drop must have occurred in a significant volume around station ELM. Other stations, such as HAT (Figure 6) do not show any clear evidence for a velocity drop at the time of the January 2010 swarm. This is reassuring in that the other paths do not primarily sample the main fault-zone and if the coda-changes were the result of a systematic shift in say source depth during the swarm, one would expect it to show up at multiple stations with similar propagation distances. It does not, indicating that the velocity change is real and confined to the portion of the fault-zone near the injection wells.

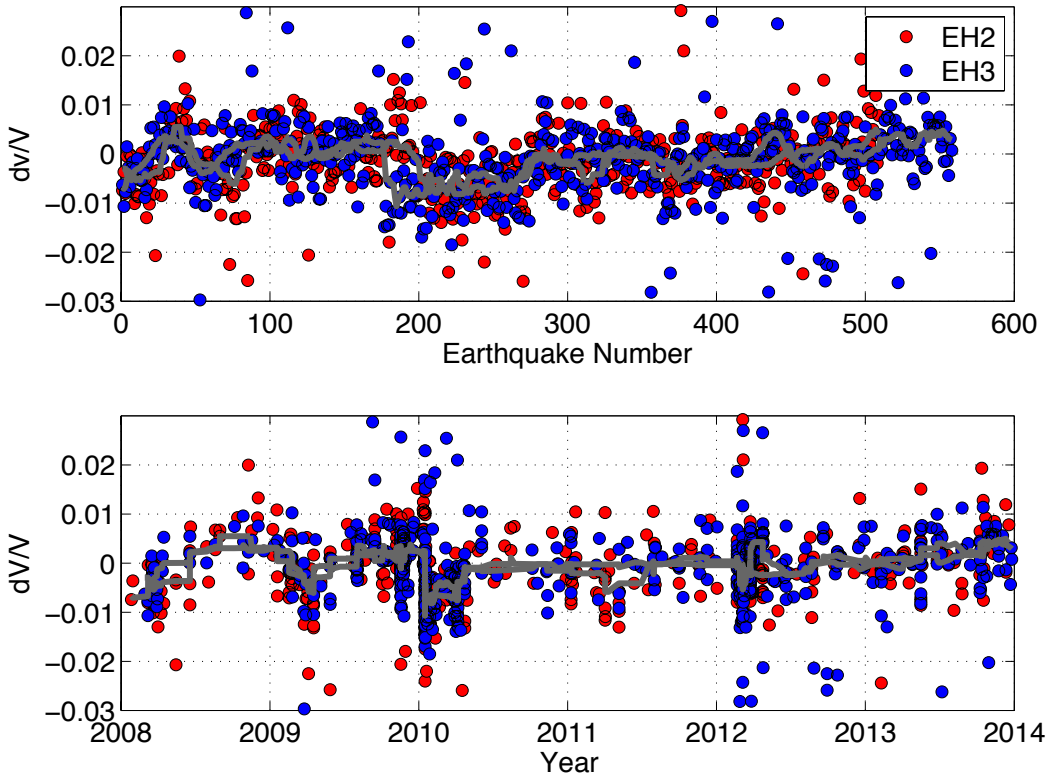

Figure 4. dV/V measurements for S-waves at ELM from a cluster of earthquakes near the injection wells in Figure 2. The top panel shows measurements on both S_wave components (EH2 and EH3) of the borehole station ELM (Figure 1 and 2). The gray lines show moving averages of the measurements from each component. The lower panel shows the same set of measurements but as a function of time. The velocity drop around earthquake #180 in the multiplet is at the beginning of a swarm in January 2010. This drop is the only major (~1%) velocity change in the 2008-2014 time period.

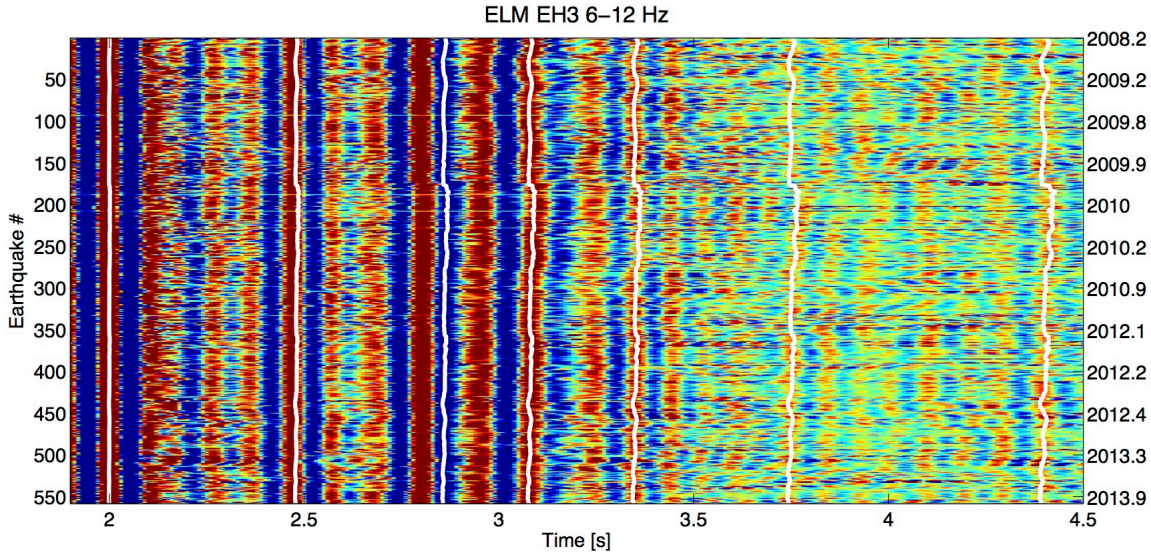

Figure 5. The S-wave coda used in the measurements in Figure 4 (colors). The white lines show the dt/T values predicted from the moving averages in Figure 4 for a few of the main coda arrivals. While the direct arrivals are continuous throught the 6 years, there is a discontinuity in the coda, particularly the late coda, around the beginning of the January 2010 swarm. This signal recovers over the course of 2010 to return to the background waveform.

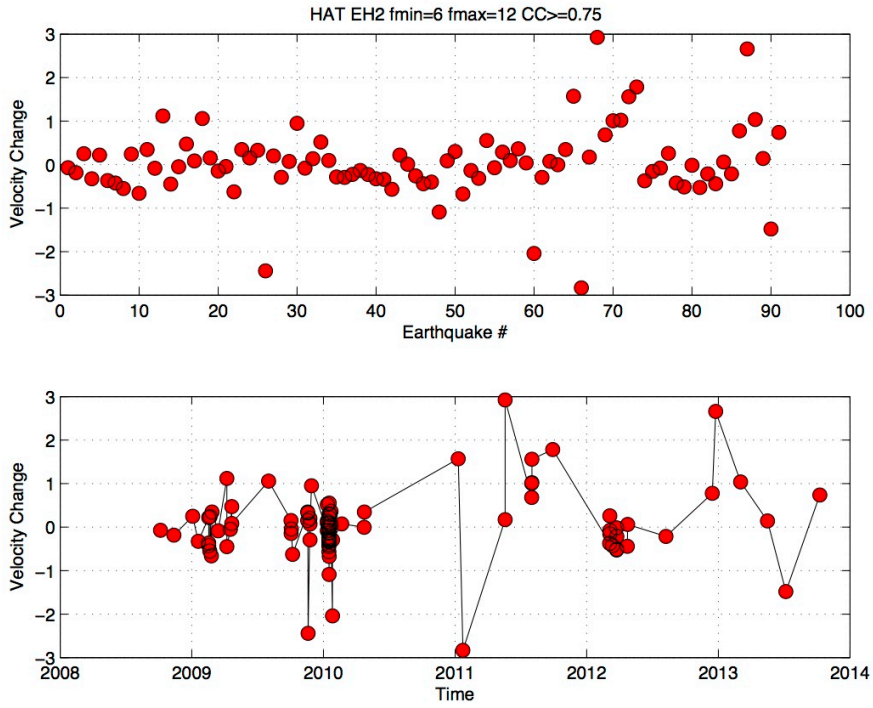

Figure 6. Similar measurements to Figure 5 but for station HAT which is further away from the earthquake swarm. Only about 1/5 of the earthquakes had sufficiently good waveforms for reliable dv/V measurements. However, it is clear that this station/path does not show a velocity drop of any significance during the 2010 or 2012 earthquake swarms.

Dissemination of Results

We have not yet written a paper on this project. I am looking for a new student to finish up the velocity change work. Most of the other stations are much more challenging than ELM to get accurate measurements on for a sufficiently dense suite of earthquakes. I hope to write a paper on this later this summer. The results discussed here waere presented at the 2015 SSA meeting by former WHOI post-doc Xiaowei Chen. She also presented her related work on earthquake source parameters (stress drop, etc) in these same swarms. She has continued this work with her new graduate students at Univ. of Oklahoma.

9) References

Chen, X., and P. M. Shearer (2011), Comprehensive analysis of earthquake source spectra and swarms in the Salton Trough, California, *J. Geophys. Res.-Solid Earth*, *116*, 17.

Chen, X., P. M. Shearer, and R. E. Abercrombie (2012), Spatial migration of earthquakes within seismic clusters in Southern California: Evidence for fluid diffusion, *J. Geophys. Res.-Solid Earth*, *117*, 7.

Clayton, R. N., L. J. P. Muffler, and D. E. White (1968), Oxygen isotope study of calcite and silicates of the River Ranch No. 1 Well, Salton Sea Geothermal Field, California, *American Journal of Science*, *266*, 968-979.

Elders, W. A., and J. H. Sass (1988), The Salton Sea Scientific Drilling Project, *J. Geophys. Res.*, *93*, 12,953-912,968.

Herzign, C. T., J. M. Mehegan, and C. E. Stelting (1988), Lithostratigraphy of the State 2-14 Borehole: Salton Sea Scientific Drilling Project, *J. Geophys. Res.*, *93*, 12,969-912,980.

Hulen, J., and F. Pulka (2001), Geology and a Working Conceptual Model of the Obsidian Butte Sector of the Salton Sea Geothermal Field, *Geothermal Resources Council Transactions*, *27*, 227-240.

Hulen, J. B., D. Kaspereit, D. Norton, W. Osborn, and F. S. Pulka (2002), Refined Conceptual Modeling and a new Resource Estimate for the Salton Sea Geothermal Field, Imperial Valley, CA, *Geothermal Resources Council Transactions*, *26*, 29-36.

Lohman, R. B., and J. J. McGuire (2007), Earthquake swarms driven by aseismic creep in the Salton Trough, California, *J. Geophys. Res.-Solid Earth*, *112*(B4), 10.

McGuire, J. J., R. B. Lohman, R. D. Catchings, M. J. Rymer, and M. R. Goldman (2015), Relationships among seismic velocity, metamorphism, and seismic and aseismic fault slip in the Salton Sea Geothermal Field region, *Journal of Geophysical Research: Solid Earth*, *120*(4), 2014JB011579.

McGuire, J. J., J. A. Collins, P. Gouedard, E. Roland, D. Lizarralde, M. S. Boettcher, M. D. Behn, and R. D. van der Hilst (2012), Variations in earthquake rupture properties along the Gofar transform fault, East Pacific Rise, *Nat. Geosci.*, *5*(5), 336-341.

Newmark, R. L., P. W. Kasameyer, L. W. Younker, and P. Lysne (1988), Shallow drilling in the Salton Sea region - The thermal anomaly, *J. Geophys. Res.*, *93*, 13,005-013,024.

Schmitt, A. K., and J. B. Hulen (2008), Buried rhyolites within the active, high-temperature Salton Sea geothermal system, *J. Volcanol. Geotherm. Res.*, *178*, 708-718.

Younker, L. W., P. W. Kasameyer, and J. D. Tewhey (1982), Geological, Geophysical, and Thermal Characteristics of the Salton Sea Geothermal Field, California, *J. Volcanology and Geothermal Research*, *12*, 221-258.